Exploring the inner structure of Titan's dunes from Cassini Radar observations

P. Sharma[1], E. Heggy[1,2] and T.G. Farr[2]

[1]Division of Geological and Planetary Sciences, California Institute of Technology, [2]Jet Propulsion Laboratory

psharma@caltech.edu

44th Lunar and Planetary Science Conference (2013)

Abstract no. 1821

INTRODUCTION

- Images taken by the Cassini Synthetic Aperture Radar (SAR), Visual and Infrared Mapping Spectrometer (VIMS) and Imaging Science Subsystem (ISS) have depicted extensive linear dune fields in Titan's equatorial regions [1,2] (Figure 1).

- Although the geomorphology of the dunes has been studied from Cassini SAR images, it has not been possible to investigate their internal structure in detail as of yet. The single polarization (HH), Ku-band (2.17cm), Cassini SAR data available for Titan [3], solely does not provide enough information to examine the shallow layering and, consequently, formation history of the dunes on Titan.

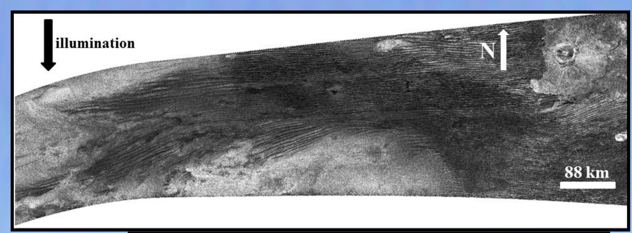
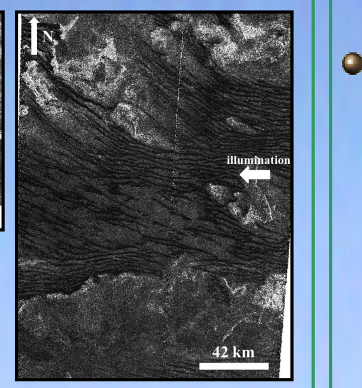

Fig. 1. Linear dunes observed in Cassini SAR images of Titan

- The purpose of this study is to qualitatively assess the internal structure, relative age and formation history of the dunes on Titan. We compare dunes on Titan to analogous terrestrial dunes in the Egyptian Sahara.

- We integrate multiple radar datasets, including SAR backscatter data for Titan's and Earth's dunes and Ground Penetrating Radar (GPR)/radar sounding data for terrestrial dunes.

- We relate the SAR backscatter variation with elevation across terrestrial dunes to the layering inferred from radar sounding data. By comparing the backscatter variation with elevation for Titanian dunes with terrestrial dunes, we can deduce the layering and inner structure of the dunes on Titan.

METHODOLOGY AND HYPOTHESIS

- GPR surveys of terrestrial linear dunes, combined with trench digging on site, have provided an insight to the aeolian layering within these features on Earth [4].

- The GPR data collected by our team provide evidence for difference in the internal layering between older (and consequently larger) and younger (and consequently smaller) dunes. GPR radargrams over individual dunes in the Siwa (left) and Qattaniya (right) dune fields in Egypt are shown in Fig. 2. Both dunes are observed to be layered in the first 8 meters of the subsurface; however, the larger dune in the Siwa dune field is much more finely layered than the smaller dune in the Qattaniya dune field, which consists of coarser internal layers.

Fig. 2 GPR radargrams at 800 MHz for Siwa (left) and Qattaniya (right) dunes in Egypt

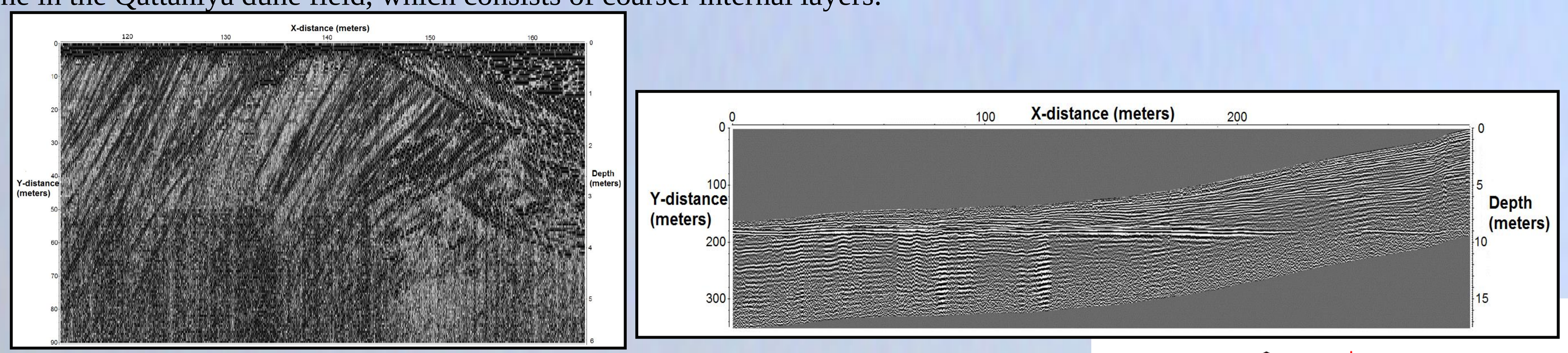

- We propose that the difference in the age and internal structure of dunes should also influence the observed surface radar backscatter (Figure 3). Older (larger) dunes with finer internal layering will exhibit a stronger dependence of radar backscatter on height along the dune profile, while the backscatter-height dependence will be much weaker or negligible for younger, smaller dunes with a coarse-layered substrate.

Fig. 3

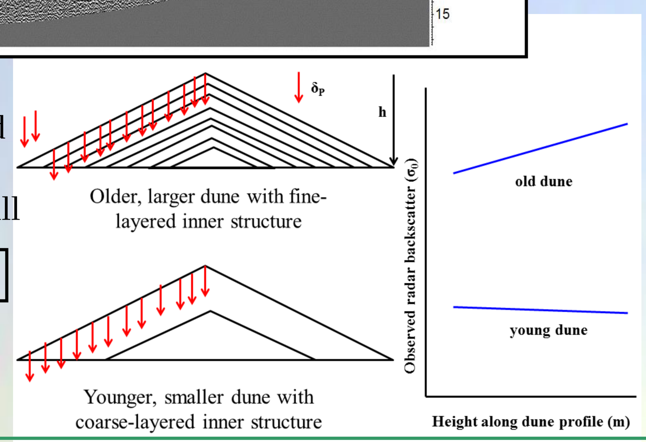

- In this study, we first validate the hypothesis stated above by examining backscatter-height variation and GPR profiles for terrestrial dunes of different ages and sizes. We then derive the backscatter-height relations for Titan's dunes and use this hypothesis to qualitatively assess their inner structure and relative ages.

TERRESTRIAL ANALOG SITES

- For comparisons with Titan's dunes, we focus on three sites having linear dune fields in the Egyptian desert: 1) Great Sand Sea in central/south-western Egypt (~26.23°N, 26.73°E), 2) Siwa dunes in north-western Egypt (~28°N, 26.17°E) and 3) Qattaniya dunes in north-eastern Egypt; west of Cairo (~30.18°N, 30.2°E) (Figure 4).

Fig. 4. Locations of three sites of analogous terrestrial linear dune fields in Egypt

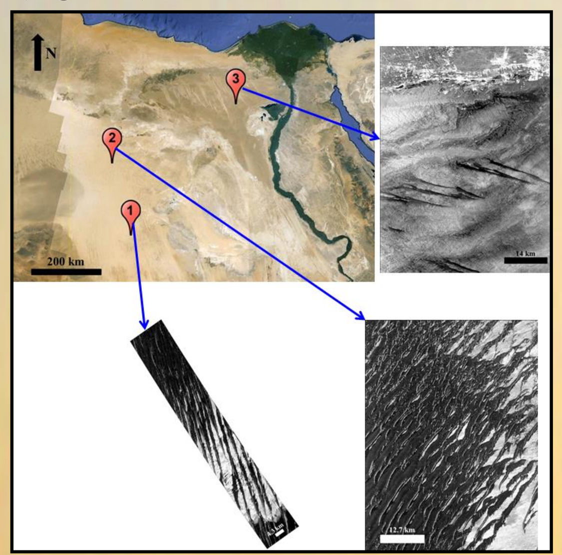

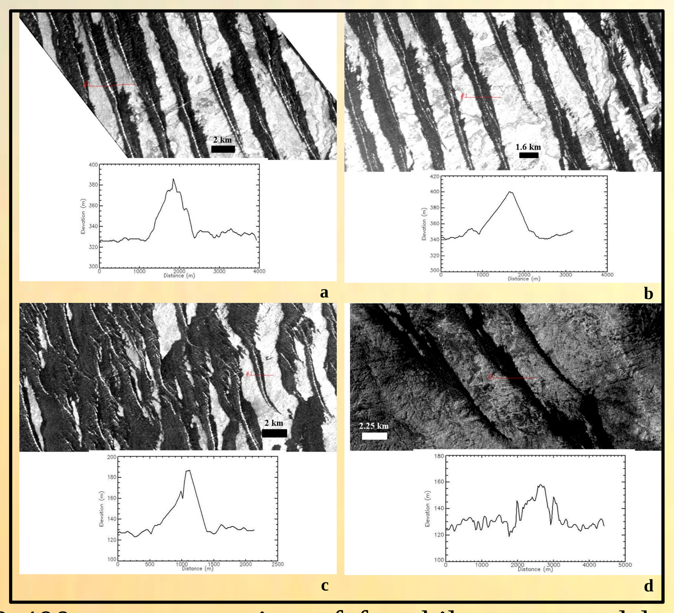

Fig. 5. SRTM elevation profiles across some example dunes in the Egyptian Sahara

- These large, linear dunes in the Egyptian desert have heights of 50-400 meters, spacing of few kilometers and lengths of ~100 km. They are thus comparable in size and morphology to the longitudinal dunes observed on Titan. Some examples of high-resolution topographic profiles of the Egyptian dunes are shown in Figure 5.

RADAR CHARACTERIZATION OF TITAN'S AND EARTH'S DUNES

- For studying the dunes on Titan, we have used backscatter data from the Cassini RADAR instrument, which is a Ku-band (13.7 GHz, 2.17 cm wavelength), linearly polarized device [3]. More than 50% of Titan's surface has been imaged by SAR. The resolution of the SAR dataset varies from ~350 m to ~1500 m.

- For our SAR characterization of the analog sites in Egypt, we used C-band (5.8cm wavelength) backscatter data from the Spaceborne Imaging Radar (SIR)-C, in Multi Look Complex (MLC) format in both quad- (HH, VV, HV and VH) and dual- (HH/HV) polarization modes, with a range resolution of 50 m and azimuth resolution of 50m [5]. We have also utilized elevation data with a resolution of 1 arc-second (~30 m) from the Shuttle Radar Topography Mission (SRTM) [6].

- We collected GPR/radar sounding data for the Qattaniya and Siwa dunes in Egypt during a site visit in September 2010 (Fig. 6). GPR data were collected using pulse repetition ground-coupled radar, operating at a central frequency of 800 MHz, with bandwidth equal to half of the central frequency, allowing 5 cm vertical resolution and a penetration depth of 8 meters into the dunes.

Fig. 6. GPR data collection during site visit to Egypt in September 2010

Analog site name	Center location coordinates	SIR-C scene PR#	SIR-C data product type and polarization	SIR-C incidence angle (°)	SRTM DEM
Great Sand Sea	26°14'02"N, 26°44'52"E	15994/15995	MLC-quad pol (HH/VV/HV/VH)	24.8	N26E026
Great Sand Sea	26°18'32"N, 26°48'10"E	15976/15977	MLC-dual pol (HH/HV)	50.381	N25E026, N26E026, N25E027, N26E027
Great Sand Sea	25°31'44"N, 27°07'30"E	16160/16161	MLC-dual pol (HH/HV)	65	N25E026, N25E027
Siwa	28°01'44"N, 26°10'58"E	15554/15555	MLC-dual pol (HH/HV)	25	N27E025, N28E025, N27E026, N28E026
Qattaniya	30°11'06"N, 30°12'03"E	46897/46898	MLC-dual pol (HH/HV)	54	N29E029, N30E029, N29E030, N30E030

Table 1. SIR-C scenes and corresponding SRTM DEMs used for terrestrial analogs

DIELECTRIC PROPERTIES OF TITAN'S DUNES

- To successfully demonstrate that the Cassini Ku-band backscatter data can provide information about sub-surface layering in the dunes on Titan, we first needed to quantify the depth to which the Cassini Ku-band microwaves can penetrate through Titan's surface.

- Based on analysis of the Cassini VIMS data, Titan's dunes consist of water ice and organics (tholins), with lesser water ice than the rest of Titan [7]. Assuming the water ice fraction for the dunes varies between 10-40%, the tholins fraction between 40-70% and the air between 20-30%, we calculated the effective dielectric constant using the Maxwell Garnet dielectric mixing law for multiphase mixtures with spherical inclusions (Eq. 1). The loss tangent and penetration depth were then calculated using Eq. 2 and 3 [8].

$$\varepsilon_{eff} = \varepsilon_e + 3\varepsilon_e \frac{\sum_{k=1}^{K} f_k \frac{\varepsilon_k - \varepsilon_e}{\varepsilon_k + 2\varepsilon_e}}{1 - \sum_{k=1}^{K} f_k \frac{\varepsilon_k - \varepsilon_e}{\varepsilon_k + 2\varepsilon_e}} \quad (1);$$

$$\text{Loss tangent} = \varepsilon''_{eff} / \varepsilon'_{eff} \quad (2);$$

$$\delta_p = \frac{\lambda_0}{4\pi}\left\{\frac{\varepsilon'_{eff}}{2}\left[\sqrt{1+\left(\frac{\varepsilon''_{eff}}{\varepsilon'_{eff}}\right)^2} - 1\right]\right\}^{-\frac{1}{2}} \quad (3)$$

- Based on these calculations, we find that the Cassini Ku-band microwaves should be able to penetrate up to ~ 3 m through Titan's surface, thus interacting with the sub-surface and providing information about layering in Titan's dunes. This implies that the shallow subsurface properties impact the observed surface radar backscatter.

VARIATION OF RADAR BACKSCATTER WITH ELEVATION ACROSS DUNES

- We used the ENVI software for processing all of the radar imaging datasets used in this study. For each site, we stacked layers of the SIR-C C-band backscatter data, SRTM elevation data and SRTM C-band backscatter data (example shown in Fig. 7).

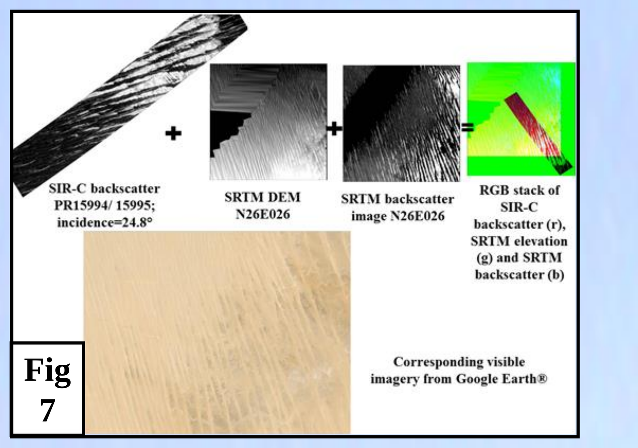

Fig 7

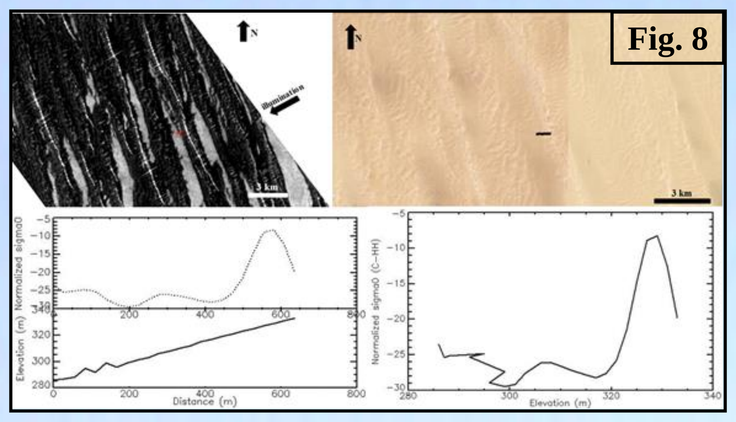

Fig. 8

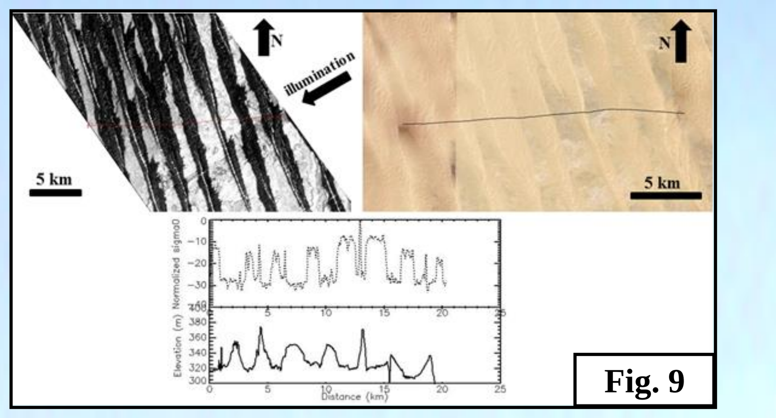

Fig. 9

- For each site, we then selected 35 profiles traversing individual dunes and extracted the corresponding backscatter and elevation data. We then examined variation of the C-band backscatter data in HH polarization with elevation across the dunes. Figures 8 and 9 show the variation of SIR-C backscatter and SRTM elevation with distance along the profile across an example individual dune and multiple dunes, respectively.

- In total, we delineated 170 profiles over terrestrial dunes in Egypt: 105 in the Great sand sea (35 each corresponding to three different incidence angles), 35 over Siwa dunes and 30 over Qattaniya dunes.

- We found that for the larger, older dunes, like the ones in the Great Sand Sea of Egypt with heights of 250-400 m or so, the backscatter shows a strong dependence on elevation, irrespective of the incidence angle. On the other hand, for smaller (50-150 m height), relatively younger dunes like the ones in the Qattaniya dune field, the backscatter shows very weak/almost no variation with elevation (Figure 10 and Table 2).

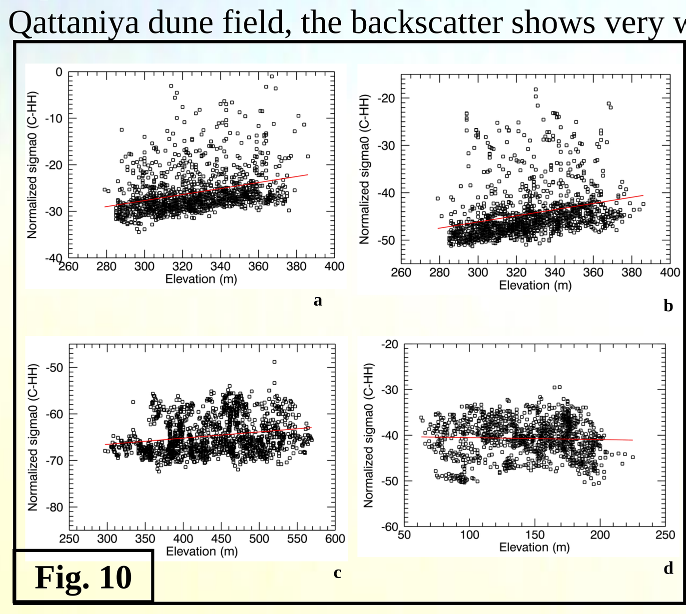

Fig. 10

Name of dune field site	Incidence angle (°)	Slope of backscatter vs. elevation relation	Intercept of backscatter vs. elevation relation	Correlation factor of backscatter vs. elevation relation	Standard deviation of slope of backscatter vs. elevation relation
Great Sand Sea (PR15994/15995)	24.8	0.065	-47.07	0.32	0.005
Great Sand Sea (PR15976/15977)	50	0.065	-65.71	0.27	0.006
Great Sand Sea (PR16160/16161)	65	0.013	-70.57	0.21	0.002
Siwa	25	0.058	-32.72	0.277	0.005
Qattaniya	54	-0.004	-40.09	0.038	0.003

Table 2. Radar backscatter v/s height dependency for terrestrial dunes

- This radar backscatter analysis confirms our hypothesis based on the GPR data, that the difference in inner structure of the dunes should affect the observed radar backscatter, with older dunes exhibiting a backscatter-height dependency different than the younger ones.

- We repeated the procedure performed for the terrestrial dunes with the four dune fields on Titan. For our analysis of backscatter versus elevation trends, we assumed dune peak heights of 50 m, 100 m and 150 m. We obtained 50 profiles from dunes in each of the four large fields on Titan, sampling 200 profiles in total. We then evaluated variation of the radar backscatter with elevation and horizontal distance across individual dunes in each of the four dune fields.

- We find dunes from all four dune fields on Titan to exhibit a very weak, almost negligible dependence of the radar backscatter on elevation (Fig. 11 and Table 3).

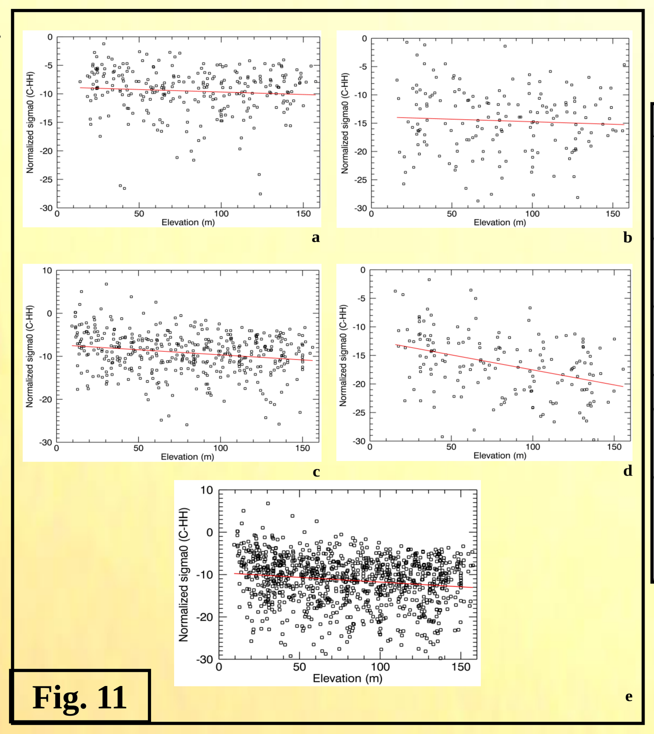

Fig. 11

		150m dune height			50m dune height			100m dune height		
Name of dune field site	Incidence angle (°)	Slope	Intercept	Correlation factor	Slope	Intercept	Correlation factor	Slope	Intercept	Correlation factor
Fensal (T17)	32-41	-0.0089	-13.85	-0.062	-0.027	-13.85	-0.062	-0.013	-13.85	-0.062
Aztlan (T25)	12-23	-0.0087	-8.81	-0.084	-0.026	-8.81	-0.084	-0.013	-8.81	-0.084
Belet (T8)	16-28	-0.023	-7.31	-0.2	-0.071	-7.31	-0.2	-0.035	-7.31	-0.2
Shangri-La (T43)	31-42	-0.052	-12.28	-0.39	-0.158	-12.28	-0.39	-0.079	-12.28	-0.39
All 4 dune fields combined	-	-0.022	-9.54	-0.16	-0.067	-9.54	-0.16	-0.034	-9.54	-0.16

Table 3. Radar backscatter versus height dependency for Titan's dunes

CONCLUSIONS

- The backscatter-height dependence exhibited by Titan's dunes is similar to the smaller terrestrial dune fields, the Qattaniya dunes, indicating coarser layering and a relatively younger age for the dunes on Titan.

- Our results indicate coarse layering in the top 3 meters of Titan's dunes, which could be the result of deposition by multiple massive dust storms in the past on Titan, which would be capable of depositing meters of organic dust. Such storms in the past would indicate fast paleo-wind regimes, resulting from large thermal gradients on Titan.

REFERENCES

[1] Lorenz, R. D. et al. (2006) Science, 312, 724-727. [2] Radebaugh, J. et al. (2008) Geomorph., 121, 122-132. [3] Elachi, C. et al. (2004) Space Sc. Rev., 115, 71-110 [4] Bristow, C.S. et al. (2000) Nature, 406, 6791, 56-59. [5] Jordan, R.L. et al. (1995) IEEE Trans. on Geo. and Remote Sens., 33, 4, 829–839. [6] Farr, T. G. et al. (2007) Rev. Geophys., 45(2), RG2004. [7] Soderblom, L. A. et al. (2007) Planetary and Space Sc., 55, 2025-2036. [8] Sihvola, A.H. (1999), Electromagnetic mixing formulas and applications. The Institution of Electrical Engineers, London, United Kingdom.